PHYSICAL REVIEW B **84**, 155310 (2011)

Momentum relaxation due to polar optical phonons in AlGaN/GaN heterostructures

J.-Z. Zhang* and A. Dyson
Department of Physics, University of Hull, Hull, HU6 7RX, United Kingdom

B. K. Ridley
School of Computing Science and Electronic Engineering, University of Essex, Colchester, CO4 3SQ, United Kingdom
(Received 5 July 2011; revised manuscript received 23 September 2011; published 17 October 2011)

Using the dielectric continuum (DC) model, momentum relaxation rates are calculated for electrons confined in quasi-two-dimensional (quasi-2D) channels of AlGaN/GaN heterostructures. Particular attention is paid to the effects of half-space and interface modes on the momentum relaxation. The total momentum relaxation rates are compared with those evaluated by the three-dimensional phonon (3DP) model, and also with the Callen results for bulk GaN. In heterostructures with a wide channel (*effective* channel width >100 Å), the DC and 3DP models yield very close momentum relaxation rates. Only for narrow-channel heterostructures do interface phonons become important in momentum relaxation processes, and an abrupt threshold occurs for emission of interface as well as half-space phonons. For a 30-Å GaN channel, for instance, the 3DP model is found to underestimate rates just below the bulk phonon energy by 70% and overestimate rates just above the bulk phonon energy by 40% compared to the DC model. Owing to the rapid decrease in the electron-phonon interaction with the phonon wave vector, negative momentum relaxation rates are predicted for interface phonon absorption in usual GaN channels. The total rates remain positive due to the dominant half-space phonon scattering. The quasi-2D rates can have substantially higher peak values than the three-dimensional rates near the phonon emission threshold. Analytical expressions for momentum relaxation rates are obtained in the extreme quantum limits (i.e., the threshold emission and the near subband-bottom absorption). All the results are well explained in terms of electron and phonon densities of states.

DOI: 10.1103/PhysRevB.84.155310 PACS number(s): 73.40.Kp, 73.63.Hs, 63.20.kd, 63.22.Np

I. INTRODUCTION

GaN-based wide-band-gap semiconductor heterostructures such as AlGaN/GaN have attracted intense research interest due to their envisaged applications in novel high-power and high-mobility devices such as heterostructure field-effect transistors (HFETs). At the interface of such a heterostructure, a two-dimensional (2D) electron gas forms due to internal spontaneous polarization plus possible strain-induced polarization by the piezoelectric effect. As the 2D electron gas (2DEG) arises in the absence of doping, impurity scattering can be minimized and high electron mobility can occur. Therefore, the electron transport in AlGaN/GaN heterostructures is determined by phonon scattering processes, which at room temperature are dominated by polar optical phonon scattering.

It is well known that the momentum relaxation rate[1] (MRR) or, equally, its inverse, the momentum relaxation time, is a key parameter for describing the dynamics of the electron transport in semiconductors under an external electric field. While it is governed by the microscopic electron-phonon scattering processes, the MRR is closely related to dynamic quantities of interest such as the electron mobility and the electron drift velocity. Hence, knowing the MRR, or more specifically its dependence on the electron energy for different AlGaN/GaN heterostructures, is fundamental to the optimization of the HFET device performance.

There have been studies of electron momentum relaxation in GaAs- and GaN-based quantum wells. For example, in an early study for GaAs quantum wells,[2] both electron scattering rates and MRRs were numerically calculated and compared with analytical results[3] obtained from the momentum conservation approximation to examine the validity of the approximation. For GaN quantum wells, Anderson *et al.*[4] studied the momentum relaxation and low-field electron transport in degenerate 2DEGs by solving a linearized Boltzmann equation. In most calculations, the polar optical phonons of the quasi-two-dimensional (quasi-2D) systems are simply taken as the longitudinal-optical (LO) phonons of the bulk material. This is referred to as the three-dimensional phonon (3DP) approximation. According to the well-established dielectric continuum (DC) model, the polar modes of a single heterostructure include half-space LO modes and interface modes, and all these modes interact with the electrons in the quasi-2D channel. Indeed, using the DC model, MRRs and mobility of electrons due to phonon absorption were calculated for AlGaN/GaN heterostructures.[5] Mori and Ando showed that the sum of the form factors associated with half-space and interface modes was equal to the form factor for bulk phonons. This implied that the *total* rates calculated with the 3DP approximation would be close to those obtained from the DC model.[1,6] However, this is only partly true, and caution should be taken in studying momentum relaxation with the 3DP approximation. The argument is as follows. First, evaluation of the MRR depends on not only the form factor, but also the electron-phonon interaction strength and detailed electron and phonon densities of states. Second, since the potential of interface modes decreases exponentially from the interface according to $e^{-q|z|}$ (Sec. II below), scattering with interface modes is weak in wide wells making the 3DP approximation a reasonable model. Indeed, for GaAs wells with widths greater than 100 Å, the 3DP model suffices for the evaluation of scattering rates[7,8] and energy loss rates.[9] For narrow wells, however, the interface phonons are important

scattering partners, and the two phonon models yield quite different rates.[8,9] However, as far as we know, there has been no comparison of MRRs based on the two phonon models. Third, the dependence of the MRR on the electron energy is of great interest. Previous scattering rate calculations[8] have shown that, when the electron energy is near to the phonon energy, the 3DP estimation becomes poorer. It is predicted that this will be true for MRRs as well. Fourth, the points above are made assuming no hot-phonon effects. In the hot-phonon regime, energy loss rates have been found to depend on the phonon models used.[6,9] MRRs are thought to do so as well.

In this paper, we study the momentum relaxation of electrons in the channels of AlGaN/GaN heterostructures. As the 3DP treatment is convenient for practical usage, one of course wants to know the discrepancy between MRRs estimated by this model and those calculated with the DC model. This comparison can be made with regard to only the total rates. On the other hand, there is an advantage of the use of the DC model in that the contributions from the quasi-2D phonon modes to the momentum relaxation rate can be singled out. Thus, it is also of great interest to find and understand behaviors of the half-space modes and interface modes in the momentum relaxation process. These are the purposes of this study. Therefore, using the two phonon models, the momentum relaxation rate is evaluated as a function of the electron kinetic energy and the *effective* channel width for the respective phonon emission and absorption processes. The MRRs from the scattering with half-space phonons and interface phonons are compared and examined, focusing on the energy dependences, the peak rates variation, and their energy shift as the heterostructure parameter (e.g., the effective channel width) is varied. We found that negative MRRs occur in all interface phonon absorption processes, and this is due to the stronger forward scattering from the long-wavelength interface modes involved. Particular attention is also paid to a comparison of the total MRRs calculated with the DC model and the 3DP approximation for a number of effective channel widths to examine the latter phonon model in the estimation of MRRs. These results are also compared with the bulk situation to find how both electron and phonon confinement and their densities of states affect the momentum relaxation.

This paper is organized as follows. In Sec. II, the dielectric continuum model for single heterostructures is briefly described where the phonon modes and associated electron-phonon interactions are given. Then, a formulation of the momentum relaxation rate in such heterostructures is presented in Sec. III. In Sec. IV, first we present results of the momentum relaxation rate in a typical AlGaN/GaN heterostructure by comparing the respective contributions to the momentum relaxation from the half-space and interface modes. Then, we show the momentum relaxation results for heterostructures with different well widths, and also compare them with the 3D bulk case. This is to investigate how quantum confinement in both electronic states and phonon modes affect the momentum relaxation. In order to examine the usual 3D phonon approximation in the evaluation of MRRs, we further compare the momentum relaxation rates obtained from the 3D phonon and DC models for a variety of AlGaN/GaN heterostructures. The phonon confinement effects on the momentum relaxation are discussed in detail. Finally, Sec. V summarizes the main results obtained. In Appendix A, a derivation of the final expressions for the MRRs is outlined for both the half-space and interface phonons. An effective numerical technique in calculating these rates is described in terms of handling the singularities of the integrals involved. It is of great interest to obtain, if at all possible, an analytical formula for the MRR in a quasi-2D system such as the heterostructure. To do this, two special cases are considered in Appendix B: (i) when the kinetic energy of the electron is sufficiently close to a phonon energy that a half-space or interface phonon can be emitted, and (ii) when the electron kinetic energy is close to zero, a phonon is absorbed. In the former case, we obtain an analytical formula for the momentum relaxation rate and, further, this rate is equal to the usual electron-phonon scattering rate. For the latter case, in contrast, we find from the obtained analytical formulas that the momentum relaxation rate is always smaller than the usual scattering rate; further, the MRR for interface phonons can have a negative value, whereas the MRR for half-space modes is always positive. These analytical expressions are used to check and interpret our numerical results.

II. OPTICAL PHONON MODES AND ELECTRON-PHONON INTERACTIONS IN THE DIELECTRIC CONTINUUM MODEL

To study the momentum relaxation in heterostructures, we need electron states, lattice vibration modes, and electron-phonon interactions. Let the interface of the heterostructure be at $z = 0$, with the barrier in the space $-L_1 < z < 0$ and the electron-containing active region in the space $0 < z < L_2$. Let $\boldsymbol{\rho} = (x, y)$ be the position vector in the plane parallel to the interface. Due to confinement in the growth direction z, the motion of an electron can be described by the wave function $\psi_{n\mathbf{k}}(\mathbf{r}) = \frac{1}{\sqrt{A}}\phi_n(z)e^{i\mathbf{k}\cdot\boldsymbol{\rho}}$, and the corresponding electron energy $E_{n\mathbf{k}} = \varepsilon_n + \mathcal{E}_{\mathbf{k}}$, where A is the sample area, n indexes the subband, and $\phi_n(z)$ is the confinement envelope function corresponding to energy ε_n. $\mathbf{k}$ is the electron wave vector parallel to the heterostructure interface, and $\mathcal{E}_{\mathbf{k}}$ is the electron kinetic energy $\mathcal{E}_{\mathbf{k}} = \hbar^2k^2/2m^*$, with m^* being the electron effective mass.

Two types of polar optical modes occur in the wurtzite structure owing to anisotropy in uniaxial crystals. The anisotropy, however, causes only a small difference in the two LO-like phonon frequencies.[10] Thus, in this study, the polar modes are simply taken to be cubiclike LO modes. In the dielectric continuum model, the polar vibration modes of a single heterostructure consist of half-space modes and interface modes.[11] The half-space modes have the frequencies of the polar modes associated with the two constituent materials with their optical vibrations, electric fields, and scalar potentials occurring in the respective constituent regions. Different from half-space modes, the interface modes have different frequencies from the polar modes of both constituent materials, and an interface mode has lattice vibrations and electric fields in both constituent regions. The barrier is a binary alloy in which the polar optical modes consist of both GaN- and AlN-like vibrations. When treating phonon modes of $Al_xGa_{1-x}N$/GaN heterostructures, we neglect all GaN-like vibrations in the alloy $Al_xGa_{1-x}N$.[12] This is based on two

considerations: (i) the half-space modes associated with the alloy have very weak interactions with electrons in the GaN channel; (ii) interface modes and their momentum relaxation rates can be dealt with in a simple way.

Let L represent the dimension of a constituent half-space in the growth direction $L = Na$, with a being the lattice constant. That is, $L = L_1$ ($L = L_2$) for the half-space of $Al_xGa_{1-x}N$ (GaN). The half-space modes then can be simply indexed by $(q_z,\mathbf{q})$, all having the LO frequency of the material $\omega_{\rm LO}$. Here, $\mathbf{q}$ is the in-plane phonon wave vector, and $q_z = n\pi/L$ ($n = 1,2,\ldots,N-1$). The Hamiltonian of an electron interacting with these half-space modes can be written as

$$\mathcal{H}_h = \sum_{\mathbf{q},q_z} \frac{\gamma_{\rm LO}}{\sqrt{2V}} \left(\frac{1}{q^2+q_z^2}\right)^{1/2} e^{i\mathbf{q}\cdot\boldsymbol{\rho}} 2\sin q_z z \times \left[a_{q_z}(\mathbf{q}) + a^+_{q_z}(-\mathbf{q})\right], \quad (1)$$

where $a_{q_z}(\mathbf{q})$ and $a^+_{q_z}(\mathbf{q})$ are the annihilation and creation operators for the half-space mode of $(q_z,\mathbf{q})$. $\gamma_{\rm LO}$ is a constant given by $\gamma^2_{\rm LO} = 2\pi e^2\hbar\omega_{\rm LO}(\frac{1}{\epsilon_\infty} - \frac{1}{\epsilon_0})$, where ϵ_0 and ϵ_∞ are the static and high-frequency dielectric constants of the constituent material, and e is the electron charge. V is the volume of the constituent region ($V = AL$). We use cgs units throughout the paper.

Let $\epsilon(\omega)$ be the lattice dielectric function in the active region $\epsilon(\omega) = \epsilon_\infty(\omega^2 - \omega^2_{\rm LO})/(\omega^2 - \omega^2_{\rm TO})$, where ϵ_∞, $\omega_{\rm LO}$, $\omega_{\rm TO}$ are the high-frequency dielectric constant, the LO and transverse optical (TO) phonon frequencies of the active region. When GaN-like vibrations are neglected, the dielectric function in the barrier is then given by $\bar\epsilon(\omega) = \bar\epsilon_\infty(\omega^2 - \bar\omega^2_{\rm LO})/(\omega^2 - \bar\omega^2_{\rm TO})$, where $\bar\epsilon_\infty, \bar\omega_{\rm LO}, \bar\omega_{\rm TO}$ are the high-frequency dielectric constant, the LO and TO phonon frequencies of AlN. The frequencies of the interface modes are determined by $\epsilon(\omega) + \bar\epsilon(\omega) = 0$, which yields two solutions ω_ν ($\nu = 1,2$; let $\omega_1 < \omega_2$). This shows that the interface phonons have no dispersion. The interface modes can be simply indexed by $(\nu,\mathbf{q})$. The electron-interface-phonon interaction Hamiltonian can be written as

$$\mathcal{H}_i = \sum_{\nu,\mathbf{q}} \frac{\gamma_\nu}{\sqrt{2A}} \frac{1}{\sqrt{q}} e^{i\mathbf{q}\cdot\boldsymbol{\rho}} e^{-q|z|} [a_\nu(\mathbf{q}) + a^+_\nu(-\mathbf{q})], \quad (2)$$

where γ_ν is given by $\gamma^2_\nu = 4\pi e^2\hbar\omega_\nu/[\beta^{-1}(\omega_\nu) + \bar\beta^{-1}(\omega_\nu)]$, with $\beta(\omega)$ and $\bar\beta(\omega)$ being dimensionless quantities, $\beta(\omega) = \frac{1}{\epsilon_\infty}\frac{(\omega^2-\omega^2_{\rm TO})^2}{\omega^2(\omega^2_{\rm LO}-\omega^2_{\rm TO})}$, $\bar\beta(\omega) = \frac{1}{\bar\epsilon_\infty}\frac{(\omega^2-\bar\omega^2_{\rm TO})^2}{\omega^2(\bar\omega^2_{\rm LO}-\bar\omega^2_{\rm TO})}$. $a_\nu(\mathbf{q})$ and $a^+_\nu(\mathbf{q})$ are the annihilation and creation operators for the interface mode $(\nu,\mathbf{q})$.

III. MOMENTUM RELAXATION RATES IN A SINGLE HETEROSTRUCTURE

By knowing the interaction Hamiltonians, the usual electron-phonon scattering rates for half-space and interface modes can be given by Fermi's golden rule. The electron momentum relaxation rate describes the response of electrons to electric fields, and can be approached by weighing the scattering rate by the appropriate decrease in momentum.[1] Let $\mathbf{k}$ be the wave vector of an electron before it is scattered by a phonon with wave vector $\mathbf{q}$, and let θ be the angle between the two 2D wave vectors. Due to momentum conservation, the emission (absorption) of the phonon causes a fractional increase of momentum of $-q\cos\theta/k$ ($q\cos\theta/k$) in the direction of $\mathbf{k}$.

Thus, the momentum relaxation rate for an electron at state $(n,\mathbf{k})$ due to emission (upper signs) or absorption (lower signs) of the half-space phonons can be written as

$$\frac{1}{\tau_h} = \frac{2\pi}{\hbar}\sum_{n',\mathbf{k}'}\sum_{q_z,\mathbf{q}} \pm\frac{q}{k}\cos\theta |\mathcal{M}_{q_z,\mathbf{q}}(n',\mathbf{k}';n,\mathbf{k})|^2 \times \left[N(\omega_{\rm LO}) + \frac{1}{2} \pm \frac{1}{2}\right]\delta(E_{n'\mathbf{k}'} - E_{n\mathbf{k}} \pm \hbar\omega_{\rm LO}), \quad (3)$$

where $\mathcal{M}_{q_z,\mathbf{q}}(n',\mathbf{k}';n,\mathbf{k})$ is the electron-phonon interaction matrix element for the electronic transition from state $(n,\mathbf{k})$ to state $(n',\mathbf{k}')$ due to the scattering with a half-space mode phonon of $(q_z,\mathbf{q})$ (frequency $\omega_{\rm LO}$), i.e., $\mathcal{M}_{q_z,\mathbf{q}}(n',\mathbf{k}';n,\mathbf{k}) = \langle n',\mathbf{k}'|\mathcal{H}_h|n,\mathbf{k}\rangle$. $N(\omega)$ is the Bose-Einstein distribution function of the phonons of frequency ω, $N(\omega) = 1/(e^{\hbar\omega/k_BT_L} - 1)$, with T_L being the lattice temperature.

Similarly, the momentum relaxation rate associated with the interface modes can be given by

$$\frac{1}{\tau_i} = \frac{2\pi}{\hbar}\sum_{n',\mathbf{k}'}\sum_{\nu,\mathbf{q}} \pm\frac{q}{k}\cos\theta |\mathcal{M}_{\nu,\mathbf{q}}(n',\mathbf{k}';n,\mathbf{k})|^2 \times \left[N(\omega_\nu) + \frac{1}{2} \pm \frac{1}{2}\right]\delta(E_{n'\mathbf{k}'} - E_{n\mathbf{k}} \pm \hbar\omega_\nu), \quad (4)$$

where $\mathcal{M}_{\nu,\mathbf{q}}(n',\mathbf{k}';n,\mathbf{k})$ are the interaction matrix elements associated with the interface modes $(\nu,\mathbf{q})$, $\mathcal{M}_{\nu,\mathbf{q}}(n',\mathbf{k}';n,\mathbf{k}) = \langle n',\mathbf{k}'|\mathcal{H}_i|n,\mathbf{k}\rangle$. Still, the upper (lower) signs are for phonon emission (absorption).

For half-space phonon scattering [Eq. (3)], each matrix element carries an integral over z, and only the matrix elements depend on q_z. Thus, summation over q_z can be simply performed for $|\mathcal{M}_{q_z,\mathbf{q}}(n',\mathbf{k}';n,\mathbf{k})|^2$. Replacing $\sum_{q_z}$ by $\frac{L}{\pi}\int_0^\infty dq_z$ and expressing the matrix element in terms of the electron and phonon envelope functions, we convert this summation $\sum_{q_z}|\mathcal{M}_{q_z,\mathbf{q}}(n',\mathbf{k}';n,\mathbf{k})|^2$ to a triple integral over q_z,z,z'. The integration over q_z can be performed analytically, reducing the triple integral to a double integral (over z, z') that yields a form factor $\mathcal{F}$ dependent on q, n, n'. Therefore, we obtain

$$\sum_{q_z}|\mathcal{M}_{q_z,\mathbf{q}}(n',\mathbf{k}';n,\mathbf{k})|^2 = \frac{\gamma^2_{\rm LO}}{A}\frac{1}{q}\mathcal{F}_{n'n}(q)\delta_{\mathbf{k}',\mathbf{k}\mp\mathbf{q}}, \quad (5)$$

with the form factor given by

$$\mathcal{F}_{n'n}(q) = \int dz\int dz'\phi^*_{n'}(z)\phi_n(z)(e^{-q|z-z'|} - e^{-q|z+z'|}) \times \phi^*_n(z')\phi_{n'}(z'), \quad (6)$$

where z, z' run through a half-space.

For interface modes, we find that the matrix elements are given by

$$|\mathcal{M}_{\nu,\mathbf{q}}(n',\mathbf{k}';n,\mathbf{k})|^2 = \frac{\gamma^2_\nu}{2A}\frac{1}{q}f_{n'n}(q)\delta_{\mathbf{k}',\mathbf{k}\mp\mathbf{q}}, \quad (7)$$

where $f_{n'n}(q)$ is the form factor

$$f_{n'n}(q) = \left|\int_{-\infty}^{\infty} dz\,\phi^*_{n'}(z)\phi_n(z)e^{-q|z|}\right|^2. \quad (8)$$

The delta function in Eq. (5) [Eq. (7)] reflects momentum conservation in the scattering of an electron with a half-space (interface) phonon. This reduces the double summation over the electron and phonon wave vectors $\mathbf{k}'$, $\mathbf{q}$ in Eqs. (3) and (4) to a single summation over either wave vector (e.g., $\mathbf{q}$), which can be transformed to an integral over the wave vector as usual. For general electron energies, however, such integrals can not be evaluated analytically, and the relaxation rates $\frac{1}{\tau_h}$, $\frac{1}{\tau_i}$ [Eqs. (3) and (4)] need to be evaluated numerically. The numerical techniques are described in Appendix A. We note that dynamic screening or antiscreening may occur, depending on electron densities (antiscreening dominates at small q, while screening is present at large q).[13,14] Following a long established approximation in the literature, here we have assumed that screening and antiscreening cancel out, and ignored screening entirely.

Actual AlGaN/GaN heterostructures reported in most experiments are strained or pseudomorphic heterostructures grown on sapphire substrates, where the 2DEG is induced by polarization charges. Self-consistent calculations[15,16] have shown that, for $Al_xGa_{1-x}N$/GaN heterostructures with various compositions x, the 2DEG densities in the lowest subband alone fit well with experimental data. The single subband model will suffice for the momentum relaxation study,[5] and in what follows, the subband index 1 will be omitted for clarity. We assume that the electrons are completely confined in a channel parallel to the interface. We model the confinement envelope function for the lowest subband by the Fang-Howard wave function[17,18]

$$\phi_1(z) = \sqrt{\frac{b^3}{2}} z e^{-bz/2}, \tag{9}$$

where b is a variational parameter that is determined by minimizing the total energy of the 2DEG system. b is related to the areal electron density N_s in the GaN channel via

$$b = \left(\frac{33\pi e^2 m^* N_s}{2\epsilon_0 \hbar^2} \right)^{1/3}. \tag{10}$$

Therefore, the form factor associated with the half-space modes is given by

$$\mathcal{F}(q) = \frac{b(8b^2 + 9bq + 3q^2)}{8(b+q)^3} - \frac{b^6}{(b+q)^6}, \tag{11}$$

and for the interface modes the form factor is

$$f(q) = \frac{b^6}{(b+q)^6}. \tag{12}$$

We note that, for *undoped* $Al_xGa_{1-x}N$/GaN heterostructures,[15,16] the electron density N_s varies with the alloy composition x to achieve a balance with the polarization and surface charges across the entire structure.[19] In the wave-function model, an effective channel width d can be defined as twice the average penetration depth of the charge in the active GaN region;[20,21] d is related to the Fang-Howard b parameter via $d = 6/b$.

In this study, the material parameters are taken from Refs. 22–24. The LO and TO phonon frequencies used for GaN are $\omega_{LO} = 91.13$ meV, $\omega_{TO} = 66.08$ meV, and for AlN we use $\omega_{LO} = 110.7$ meV, $\omega_{TO} = 76.1$ meV. The high-frequency dielectric constants are taken to be 5.29 and 4.68 for bulk GaN and AlN, respectively. The electron effective mass for GaN is $m^* = 0.22m_0$ (m_0 is the free electron mass). The temperature is fixed at room temperature 300 K, and hot-phonon effects are not considered. Calculations are performed for a variety of AlGaN/GaN heterostructures by varying the value of the electron density. For numerical integration in q space (see Appendix A), 155 Gauss-Legendre quadrature points are used and excellent convergence is achieved.

IV. RESULTS AND DISCUSSIONS

Scattering rates and momentum relaxation rates are usually given for convenience in units of a basic rate W_0 (Ref. 25) relating to bulk parameters $W_0 = \frac{e^2}{\hbar}\sqrt{2m^*\omega_{LO/\hbar}}(\frac{1}{\epsilon_\infty} - \frac{1}{\epsilon_0})$. W_0 is 142 THz for bulk GaN, which is approximately 17 times higher than the W_0 value for bulk GaAs (the latter semiconductor has smaller electron effective mass and optical phonon frequencies). We first look at momentum relaxation rates calculated using the dielectric model. The optical phonons contributing for the momentum relaxation are the GaN half-space modes ($\hbar\omega_{LO} = 91.13$ meV), and the lower- and higher-energy interface modes ($\hbar\omega_1 = 69.70$ and $\hbar\omega_2 = 102.09$ meV, respectively). We first choose a heterostructure with an effective well width of 50 Å (corresponding to an electron density of $N_s = 10^{13}/\text{cm}^2$), and shall discuss later what happens to the momentum relaxation when the well width varies. We separate half-space modes from interface modes and compare their respective contributions to the momentum relaxation rate. Figure 1 shows the calculated momentum relaxation rates in units of W_0 as a function of the electron kinetic energy due to the emission of the half-space modes of GaN

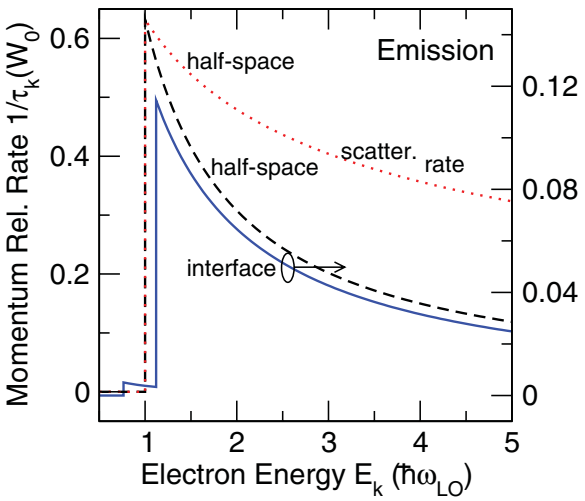

FIG. 1. (Color online) Momentum relaxation rates from the *emission* of half-space modes (dashed line) and interface modes (solid line, against the right y axis) as a function of kinetic energy for an electron in the lowest subband of a single AlGaN/GaN heterostructure with an effective well width of 50 Å (see text). The dotted curve represents the electron scattering rate due to the *emission* of half-space phonons. The momentum relaxation rates and scattering rates are in units of W_0 (see text) and the electron kinetic energy is made dimensionless with respect to the LO phonon energy $\hbar\omega_{LO}$ of bulk GaN.

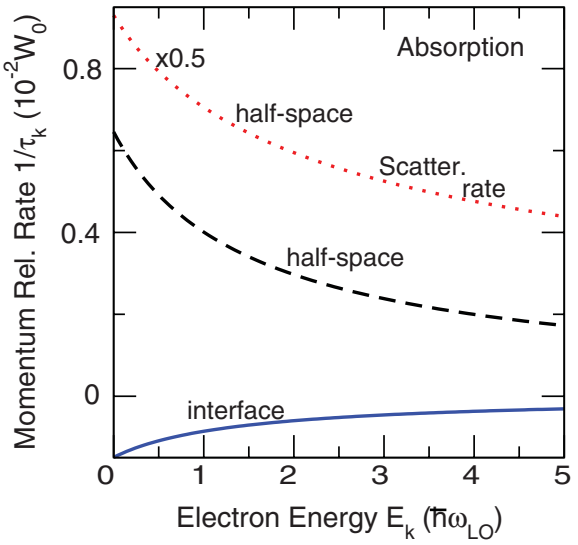

FIG. 2. (Color online) Momentum relaxation rates vs electron kinetic energy due to the *absorption* of half-space phonons (dashed line) and interface phonons (solid line). The dotted curve shows the electron scattering rate (×0.5) due to the *absorption* of half-space modes. Other notations are the same as in Fig. 1.

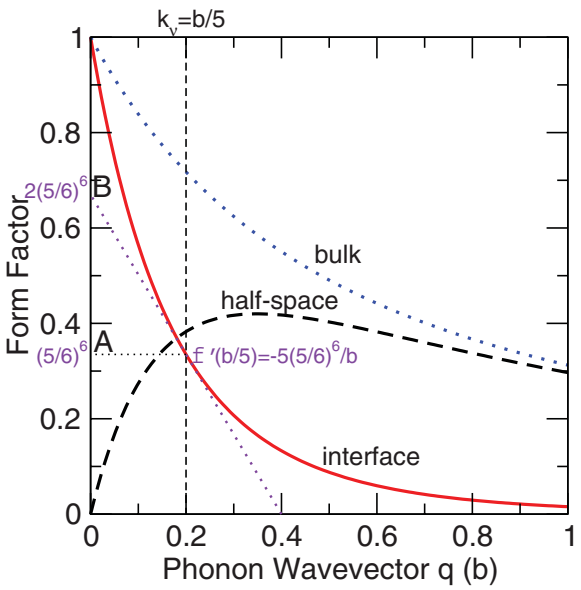

FIG. 3. (Color online) Form factors associated with the electron-phonon interactions vs the dimensionless phonon wave vector for half-space (dashed curve), interface (solid curve), and bulk modes (dotted curve). The electron is in the lowest subband, the confinement envelope function of which is modeled by the Fang-Howard wave function. The diagram shows an analytical MRR solution due to interface phonon absorption at $k \to 0$. Zero MRR occurs when the critical wave vector k_ν is equal to $b/5$ (dashed vertical line). The tangent line (dotted oblique line) to the form-factor curve at the point $[b/5,(5/6)^6]$ intersects the vertical axis at the point B, $|AB| = |OA|$. The slope of the tangent is $f'(b/5) = -5(5/6)^6/b$.

(dashed line) and the interface modes (solid line, against the right y axis). For clarity, the dimensionless electron energies are introduced with reference to the bulk GaN LO phonon energy $\hbar\omega_{\rm LO}$. Abrupt threshold emission occurs at $\hbar\omega_{\rm LO}$ for half-space modes and at $\hbar\omega_1$, $\hbar\omega_2$ for interface modes. In particular, since the interface modes have two frequencies, the momentum relaxation rate displays two clear discontinuities at the two energies $\hbar\omega_1, \hbar\omega_2$ as expected. The half-space modes dominate the momentum relaxation. For instance, the peak rate at $\hbar\omega_{\rm LO}$ is approximately six times that at the higher interface phonon energy $\hbar\omega_2$. It is interesting to note that, at the threshold for half-space or interface mode emission, analytical expressions exist for the momentum relaxation rate, and further this rate is equal to the usual electron-phonon scattering rate (a proof of this is presented in Appendix B). This is illustrated in Fig. 1, where the electron scattering rate due to the half-space modes is also shown (dotted line). In fact, the analytical solution provides a good criterion for a check of our numerical result. By substituting the material parameters into Eq. (B1), one obtains the theoretical rate for threshold $(\frac{1}{\tau_h})_{\rm th} = 0.631\,789\,743 W_0$. Numerical calculation of $\frac{1}{\tau_h}$ as given by Eq. (A9) with $\mathcal{E}_{\mathbf{k}}/\hbar\omega_{\rm LO} = 1 + 10^{-10}$ yields a rate of $0.631\,789\,784 W_0$, showing that an accurate calculation has been achieved.

We now turn to phonon absorption. The results of the rates are shown in Fig. 2 (well width of 50 Å). Clearly, the MRRs for both half-space and interface modes vary continuously with the electron kinetic energy. There is no special electron energy where rates of momentum relaxation and scattering coincide, and the scattering rates are always faster than the MRRs for both half-space and interface phonons (compare the rates, for example, for half-space modes, namely, the dashed and dotted curves in Fig. 2). We checked numerically that this is true also for heterostructures with different well widths. These are quite different from the phonon emission case above. In fact, in the limiting $k \to 0$ case where analytical solutions exist, it can be proved that the scattering rate is always larger than the MRR for half-space and interface modes (Appendix B). Furthermore, in the phonon absorption case, interestingly the MRR from the interface modes is negative and approaches zero as the electron energy increases (solid line in Fig. 2). This can be explained as follows. According to the expression for the fractional increase of momentum [Eq. (A1)], in a phonon absorption process, the phonon wave vector q and the phonon energy $\hbar\omega_\nu$ counteract each other in changing the crystal momentum: the former decreases the momentum through backward scattering, while the latter increases the momentum by forward scattering. Let k_ν denote the electron wave vector for threshold emission of an interface phonon of frequency ω_ν to occur, that is, $k_\nu = \sqrt{2m^*\omega_\nu/\hbar}$. At a particular electron energy ($\mathcal{E}_{\mathbf{k}} \neq 0$), the momentum relaxation occurs due to the absorption of all the interface phonons with wave vectors $q \in [q_\nu^-, q_\nu^+]$ [Eq. (A6)]: As $q_\nu^- < k_\nu < q_\nu^+$, the interface modes of $q < k_\nu$ contribute a negative MRR, whereas the modes of $q > k_\nu$ make a positive contribution. For interface modes, their interaction with the electron in the lowest subband is very different from the interaction of half-space modes. Since the derivative of the form factor is $f'(q) = -6f(q)/(b+q) < 0$, the electron-interface phonon interaction decreases *faster* at smaller phonon wave vectors q, as is seen from the form factor in Fig. 3 (the form factors of the half-space modes and bulk modes are also shown for comparison). Thus, when the contribution of the $q < k_\nu$ modes dominates, a negative MRR

occurs. It is understood that the higher-frequency modes are more likely to cause a negative MRR. We have checked and found that, indeed, the negative MRRs in Fig. 2 are mostly due to the higher-frequency interface modes. These rates, however, have a smaller magnitude than the half-space mode rates (because of the larger density of states of half-space modes), so the total rates remain to be positive. Negative total MRRs have been found to occur in one-dimensional systems[25,26] where forward scattering processes dominate.

In the special case $k \to 0$, the MRR can be obtained analytically (Appendix B) and the rate due to *absorption* of the ω_ν interface phonons is proportional to $1 + k_\nu f'(k_\nu)/f(k_\nu) = (b - 5k_\nu)/(b + k_\nu)$ [see Eqs. (B4) and (B6)]. For a negative MRR to occur, therefore, the logarithmic derivative of $f(k_\nu)$ multiplied by the critical wave vector k_ν must be smaller than -1, or simply $k_\nu > b/5$. This further proves that it is the *rapid* decrease in the form factor that causes the negative MRR. This analytical solution can be clearly represented using a geometric diagram as shown in Fig. 3. Consider first $k_\nu = b/5$. Let us draw a tangent line to the form factor curve at the point $[b/5,(5/6)^6]$. With the slope of $f'(b/5) = -5(5/6)^6/b$, this tangent intersects the vertical axis at the point with ordinate $f(b/5) - \frac{b}{5} f'(b/5) = 2(5/6)^6$, exactly twice the $f(b/5)$ value and making the derivative term contribution balance with that of the form-factor term (this balance is given by $|AB| = |OA|$ in Fig. 3). That is, zero MRR occurs at $k_\nu = b/5$. When $k_\nu > b/5$, one has $|AB| > |OA|$, i.e., the derivative term $k_\nu f'(k_\nu)$ is larger in magnitude than the form factor $f(k_\nu)$, then the momentum relaxation rate becomes negative. For the lower- and higher-frequency interface modes, the k_ν values are 0.06 and 0.08 Å^{-1}, respectively, and one verifies that, in the 50-Å well, indeed $k_\nu > b/5 = 0.024$ Å^{-1}, and a negative rate due to the interface phonons occurs (Fig. 3). To have a positive rate, on the other hand, one needs to raise the electron density N_s and, consequently, the b value according to Eq. (10); this requires that $N_s > 500\epsilon_0\omega_\nu{}^{3/2}\sqrt{2m^*\hbar}/(33\pi e^2)$. That is, it is required that $N_s > 1.5$, 2.7×10^{14}/cm^2 corresponding to the lower and higher frequencies ω_1, ω_2. These values are unacceptably larger than the known electron density values of AlGaN/GaN heterostructures.[15,16,27] Therefore, the small-k rates are negative at realistic electron densities for both the ω_1 and ω_2 phonons (as shown in Fig. 4).

We now investigate how MRRs vary with the electron density or, equally, the well width. In a single heterostructure, the width of the triangular well is determined by the 2DEG density;[20] the higher the density is, the narrower the well is. In the Fang-Howard wave-function model we use here, changing the electron density will change the value of b [Eq. (10)] and therefore alter the effective well width d ($d = 6/b$). To see how MRRs vary with the well width, calculations were performed for AlGaN/GaN heterostructures at a number of electron densities. It is estimated that degeneracy will become important for electron densities in excess of 8×10^{12} cm^{-2}. Compared with the nondegenerate case, it means that, at room temperature, more electrons will have the energy to emit phonons, but the effect of this will be reduced by the occupancy of the lower state inhibiting the emission. Nevertheless, it will be true that the energy range over which the interaction occurs will be generally higher, which, following the well-known property of the interaction with polar modes, will result in weakening the interaction strength. Figure 5 illustrates the results for three electron densities 10^{11}, 10^{13}, 5×10^{13} cm^{-2} (corresponding to the effective well widths of 215, 50, and 30 Å, respectively). The MRRs shown here are the *total* rates due to the emission and absorption of all half-space and interface modes. The bulk result calculated from the

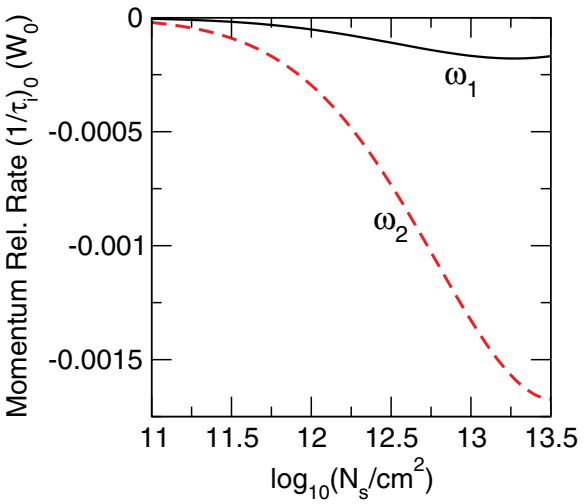

FIG. 4. (Color online) The momentum relaxation rates at $k \to 0$ due to absorption of lower- (ω_1) and higher-frequency (ω_2) interface phonons as functions of the common logarithm of the electron density in cm^{-2}.

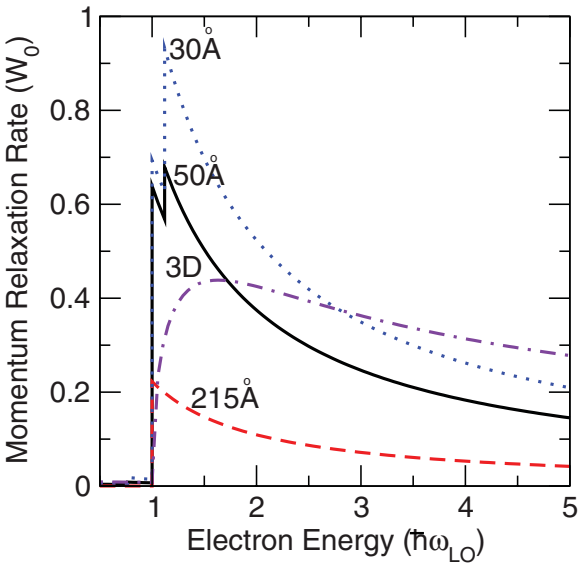

FIG. 5. (Color online) Total momentum relaxation rates vs electron kinetic energy obtained from the dielectric continuum model for three single AlGaN/GaN heterostructures of effective well widths 215 Å (dashed line), 50 Å (solid line), and 30 Å (dotted line). The bulk GaN result calculated with the Callen formula is also shown (dot-dashed line). The effective well widths of these single AlGaN/GaN heterostructures are determined by the areal electron densities in the channels: the well width of 215 Å corresponds to the electron density of 10^{11}/cm^2, well width 50 Å corresponds to electron density 10^{13}/cm^2, and well width 30 Å corresponds to electron density 5×10^{13}/cm^2.

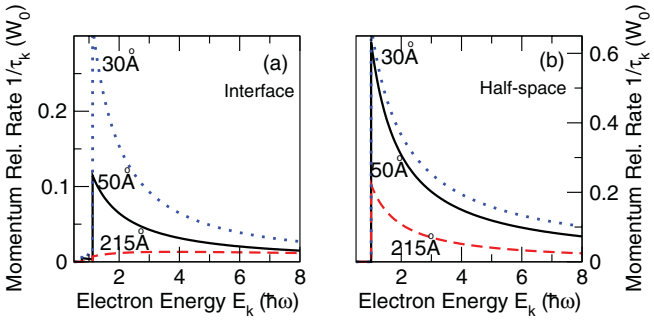

FIG. 6. (Color online) Momentum relaxation rates from the emission of (a) interface and (b) half-space phonons for the three single AlGaN/GaN heterostructures as specified in Fig. 5. The rate values from interface modes for the 215-Å well have been enlarged by 10 times.

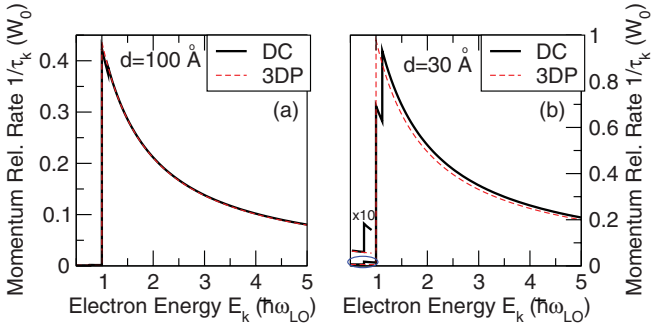

FIG. 7. (Color online) Total momentum relaxation rates vs electron kinetic energy calculated from the dielectric continuum (DC) model and the three-dimensional phonon (3DP) approximation as labeled for two single AlGaN/GaN heterostructures of effective well widths (a) 100 and (b) 30 Å. In (b), the rates for energies just below the LO phonon energy have been enlarged by 10 times for clarity.

Callen formula is also shown for comparison. We see that as the electron density increases (i.e., the well narrows), the MRRs increase; in particular, the high-rate portion just above the emission threshold increases fast, its energy region being widened from the half-space LO energy $\hbar\omega_{\rm LO}$ to the higher-frequency interface phonon energy $\hbar\omega_2$. Further, in narrow wells, interestingly, the dominant momentum relaxation rates can exceed those in bulk GaN. However, the MRRs decrease rapidly with the electron kinetic energy so we see that the rates in all the wells are smaller than the corresponding bulk values at high electron energies. To find the cause, we need to separate and check contributions to the MRRs from the interface and the half-space modes, respectively. We do so for the phonon emission case only, as the rates due to the phonon absorption are very small. In Figs. 6(a) and 6(b), we show the MRRs from the interface modes and the half-space modes, respectively, for the three electron densities above. Clearly, in the wide well (215 Å), the rates from interface modes are two orders of magnitude smaller than those from half-space modes, and thus only the abrupt feature from the half-space modes is visible in Fig. 5 (dashed line). As the well narrows, both the rates from the interface modes and those from the half-space modes increase, but the former increase rapidly. For instance, in the narrow well (30 Å), the peak rate from the higher-frequency interface modes has reached approximately half that from the half-space modes. This is again due to the different electron-phonon interactions for interface and half-space modes, as is reflected by the wave-vector dependences of their form factors: the form factor of the interface modes decreases monotonically, and the decrease becomes slower as the well narrows. This causes interface phonons to become increasingly important in narrow wells. Therefore, the sharp features from both half-space and interface modes appear on the total rate curve (solid and dotted lines, Fig. 5). At high electron energies, the quasi-2D system has smaller electronic density of states than bulk, resulting in slower 2D rates than 3D rates. We note that the 2D rates at the three emission thresholds $\hbar\omega_1$, $\hbar\omega_2$, $\hbar\omega_{\rm LO}$ are all finite, which is different from the situation in bulk where the zero rate occurs at the emission threshold $\hbar\omega_{\rm LO}$. This has been explained in Ref. 2: In the quasi-2D system, the density of states associated with the final states of the electronic transitions is finite, while its counterpart in 3D is zero.

The 3DP approximation has been widely used to study carrier-phonon interactions as well as evaluate carrier-phonon scattering rates and electron momentum relaxation rates for quasi-2D semiconductor systems.[2,3,25,28] Here, we compare momentum relaxation rates in AlGaN/GaN heterostructures calculated with the DC and 3DP models. To do this, we show in Figs. 7(a) and 7(b) the results of MRRs for a wide well (100 Å) and narrow well (30 Å), respectively. For the wide well, the two phonon models yield literally the same momentum relaxation rates, the two lines being virtually coincident in Figs. 7(a). This is explained as follows. The potential of the interface modes decreases exponentially according to $e^{-q|z|}$ [Eq. (2)]. The average value of the position for electrons is $z_{\rm av} = 50$ Å. For the higher- and lower-frequency interface phonons, the characteristic wave vector k_ν is 0.06 and 0.08 1/Å, making $k_\nu z_{\rm av} = 3,4$, respectively. Thus, the effect of the interface modes can be neglected. In the narrow well, the MRRs calculated from the two phonon models are quite different at electron energies around the optical phonon energies: the DC model yields higher rates below $\hbar\omega_{\rm LO}$, due to significant scattering from the lower-frequency interface phonons, whereas the 3DP rates are significantly higher above $\hbar\omega_{\rm LO}$ but become smaller beyond $\hbar\omega_2$ than those obtained from the DC model. The 3DP model underestimates the MRRs just below $\hbar\omega_{\rm LO}$ by 70% and overestimates the rates just above $\hbar\omega_{\rm LO}$ by about 40%. At further high electron energies, the two models give similar rates. This is again because the interface phonon scattering becomes increasingly important in narrow wells. The effect above becomes more pronounced as the well width is further reduced. However, only wells wider than 10 Å have been considered since the effective mass approximation breaks down below this. We note that our results [Figs. 7(a) and 7(b)] are consistent with a conservation rule for optical phonon scattering in heterostructures,[29] and this shows that the rule can be extended to momentum relaxation rates.

V. CONCLUSIONS

In conclusion, using the dielectric continuum model, we studied momentum relaxation for quasi-2D electrons in

AlGaN/GaN heterostructures. We found that half-space phonon scattering dominates the momentum relaxation processes due to the large density of states of half-space modes. For interface phonons, negative momentum relaxation rates occur in the phonon absorption processes. This stems from the peculiar electron-interface-phonon interaction that decreases *rapidly* as the wave vector increases, thus causing stronger forward scattering than the backward scattering. Our evaluation predicts that this negative rate will occur in normal AlGaN/GaN heterostructures with electron densities under $10^{14}/\text{cm}^2$. Further, we examined the three-dimensional phonon model by comparing the total momentum relaxation rates calculated with the two phonon models. We found that the 3DP phonon model is generally a good approximation for AlGaN/GaN heterostructures with a wide channel (>100 Å). Interface phonons in the DC model, on the other hand, become important in electron momentum relaxation for only narrow-channel heterostructures, with distinctive features associated with abrupt threshold emission appearing on the rate curves. For a 30-Å GaN channel, for instance, we found that the 3DP model underestimates the MRRs just below the bulk phonon energy by 70%, and overestimates the rates just above the bulk phonon energy by 40%. We also compared these quasi-2D rates with results for bulk GaN calculated from the Callen formula. We found that, in narrow-channel heterostructures, the quasi-2D rates have very large peak values compared to the 3D rates, but become smaller at high electron kinetic energies. To interpret numerical results, we also obtained transparent expressions for momentum relaxation rates for two limiting cases, namely, the threshold emission and the near subband-bottom absorption. We discussed the results in terms of electron and phonon densities of states.

ACKNOWLEDGMENTS

The authors would like to thank the Office of Naval Research, US, for funding under the Grant No. N00014-09-1-0777 sponsored by P. Maki.

APPENDIX A: NUMERICAL CALCULATION OF ELECTRON MOMENTUM RELAXATION RATES IN A SINGLE HETEROSTRUCTURE

We first consider interface phonon scattering. In order to emit an interface phonon of frequency ω_ν ($\nu = 1,2$), the electron in the lowest subband must have sufficient kinetic energy, that is, $\mathcal{E}_\mathbf{k} \geqslant \hbar\omega_\nu$. This defines a wave vector k_ν: $k_\nu = \sqrt{2m^*\omega_\nu/\hbar}$. This wave vector is a key parameter in electron and phonon wave-vector space, and will be frequently used for our description and numerical calculation of momentum relaxation. Its significance will be apparent shortly.

According to conservation of both energy and momentum, the fractional increase of momentum is given by[1]

$$\mp\frac{q}{k}\cos\theta = -\frac{1}{2}\left[\left(\frac{q}{k}\right)^2 \pm \frac{\hbar\omega_\nu}{\mathcal{E}_\mathbf{k}}\right] = -\frac{1}{2k^2}\left(q^2 \pm k_\nu^2\right) \quad \text{(A1)}$$

when an interface phonon of frequency ω_ν is emitted (upper signs) or absorbed (lower signs). Clearly, the fractional increase of momentum for phonon emission is always negative, indicating that the momentum projection on the original electron wave vector $\mathbf{k}$ is decreased after a phonon is emitted. In the phonon absorption case, on the other hand, the fractional increase of momentum can be positive or negative, depending on the strength of the forward scattering $\hbar\omega/\mathcal{E}_\mathbf{k}$ relative to that of the backward scattering $(q/k)^2$.

For any given k ($k \neq 0$), limitations on the phonon wave vector q are imposed again by the requirement of conservation of energy and momentum. These can be sought in a similar way to those in bulk semiconductors.[1] The minimum and maximum interface phonon wave vectors are given by

$$q_\nu^- = k\left(1 - \sqrt{1 - \frac{k_\nu^2}{k^2}}\right), \quad \text{(A2)}$$

$$q_\nu^+ = k\left(1 + \sqrt{1 - \frac{k_\nu^2}{k^2}}\right) \quad \text{(A3)}$$

for phonon emission, and

$$q_\nu^- = k\left(\sqrt{1 + \frac{k_\nu^2}{k^2}} - 1\right), \quad \text{(A4)}$$

$$q_\nu^+ = k\left(\sqrt{1 + \frac{k_\nu^2}{k^2}} + 1\right) \quad \text{(A5)}$$

for phonon absorption. In both cases, one finds that $q_\nu^- < k_\nu < q_\nu^+$.

To calculate the momentum relaxation rate $1/\tau_i$ from interface phonon scattering, we insert the fractional increase of momentum [Eq. (A1)] together with the interaction matrix elements for interface modes [Eq. (7)] into Eq. (4). For intra-subband scattering, the energy terms in the δ function simplify to $\mathcal{E}_{\mathbf{k}'} - \mathcal{E}_\mathbf{k} \pm \hbar\omega_\nu$. Further, the wave-vector δ function $\delta_{\mathbf{k}',\mathbf{k}\mp\mathbf{q}}$ is used to remove the summation over the electron wave vector $\mathbf{k}'$. By converting the summation over the phonon wave vector $\mathbf{q}$ to an integral and integrating over angle, we then obtain

$$\frac{1}{\tau_i} = \frac{m^*}{2\pi\hbar^3}\sum_\nu \frac{\gamma_\nu^2}{k}\left[N(\omega_\nu) + \frac{1}{2} \pm \frac{1}{2}\right]\int_{q_\nu^-}^{q_\nu^+}\frac{dq}{q}f(q)\frac{1}{2k^2} \times \left(q^2 \pm k_\nu^2\right)\left\{1 - \left[\frac{1}{2}\frac{k_\nu}{k}\left(\frac{q}{k_\nu} \pm \frac{k_\nu}{q}\right)\right]^2\right\}^{-1/2}. \quad \text{(A6)}$$

This rate expression shows that k_ν has a clear physical meaning; that is, it is a *critical* wave vector for the evaluation of the momentum relaxation rate contributed from all allowed phonon *absorption* processes: the $q < k_\nu$ phonon processes contribute a negative value to the rate, while the $q > k_\nu$ phonon processes make a positive contribution, and the net rate is simply their sum.

The integral appearing in Eq. (A6) is dimensionless and denoted by I_ν for simplicity. To calculate this integral, we need to know the properties of its integrand. Let the quantity in the latter square brackets be $\xi(q)$, a function of variable q for a given k: $\xi(q) = \frac{1}{2}\frac{k_\nu}{k}\left(\frac{q}{k_\nu} \pm \frac{k_\nu}{q}\right)$. In the phonon emission case, the function $\xi(q)$ has the minimum value of $\frac{k_\nu}{k}$ at $q = k_\nu$, and increases smoothly to the maximum value 1 at both limits of integration q_ν^-, q_ν^+. This is illustrated in Fig. 8(a)

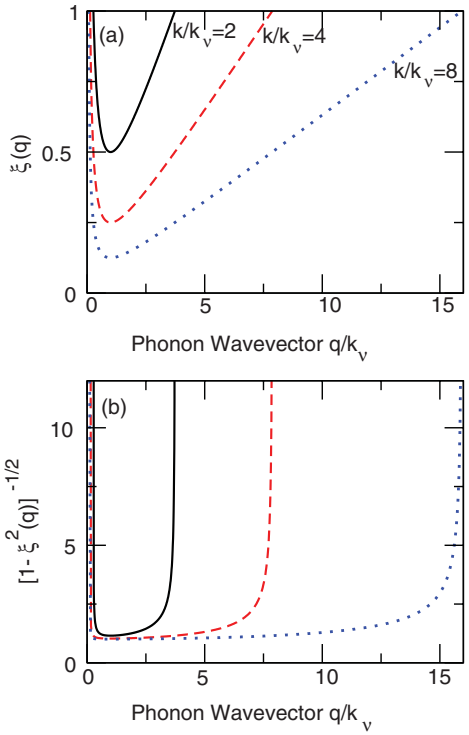

FIG. 8. (Color online) Two dimensionless quantities (a) $\xi(q) = \frac{1}{2}\frac{k_\nu}{k}(\frac{q}{k_\nu} + \frac{k_\nu}{q})$ and (b) $[1-\xi^2(q)]^{-1/2}$ in the integrand for numerical integration [see Eq. (A6) and Appendix A for detail] as a function of the dimensionless phonon wave vector q/k_ν for three k values: $k/k_\nu = 2,4,8$. Here, k is the magnitude of the two-dimensional electron wave vector, and k_ν is the characteristic electron wave vector for the threshold phonon emission.

for three k values: $k/k_\nu = 2$, 4, 8. As a result, the function $[1-\xi^2(q)]^{-1/2}$ and, hence, the integrand of I_ν go to $+\infty$ at both limits of q {Fig. 8(b) shows the function $[1-\xi^2(q)]^{-1/2}$ for the three k values above}. In the phonon absorption case (not shown), the function $\xi(q)$ displays different behavior; it increases monotonically from -1 at $q = q_\nu^-$, through 0 at k_ν, finally to 1 at q_ν^+. This again causes $[1-\xi^2(q)]^{-1/2}$ and the integrand to approach $+\infty$ at the two limits of q. Accurate evaluation of the integrals I_ν is important in obtaining the correct momentum relaxation rates. On the other hand, the calculation should be efficient as all interface and half-space modes are involved, and a large electron wave-vector space is to be sampled. Therefore, the singularities of the integrals need to be properly treated.

In what follows, the treatment is illustrated for phonon emission, but the phonon absorption case can be dealt with analogously. If we use $G(q)/\sqrt{1-\xi(q)}$ to represent the integrand of I_ν, clearly, $G(q)$ is a regular function of phonon wave vector $q \in [q_\nu^-, q_\nu^+]$. Having known the properties of the integrand, we can use k_ν conveniently to partition the integral into two parts over the intervals $[q_\nu^-, k_\nu]$ and $[k_\nu, q_\nu^+]$, respectively, such that each part contains only one singularity at q_ν^- or q_ν^+. That is,

$$I_\nu = \int_{q_\nu^-}^{k_\nu} \frac{G(q)}{\sqrt{1-\xi(q)}}dq + \int_{k_\nu}^{q_\nu^+} \frac{G(q)}{\sqrt{1-\xi(q)}}dq. \tag{A7}$$

Then, we transform the integrals on the right-hand side into

$$\begin{aligned} I_\nu = &\int_{q_\nu^-}^{k_\nu} \frac{G(q)-\zeta(q)G(q_\nu^-)}{\sqrt{1-\xi(q)}}dq + G(q_\nu^-)\int_{q_\nu^-}^{k_\nu} \frac{\zeta(q)}{\sqrt{1-\xi(q)}}dq \\ &+ \int_{k_\nu}^{q_\nu^+} \frac{G(q)-\eta(q)G(q_\nu^+)}{\sqrt{1-\xi(q)}}dq \\ &+ G(q_\nu^+)\int_{k_\nu}^{q_\nu^+} \frac{\eta(q)}{\sqrt{1-\xi(q)}}dq. \end{aligned} \tag{A8}$$

The functions $\zeta(q)$ and $\eta(q)$ are chosen such that the limits $\lim_{q\to q_\nu^-}[G(q)-\zeta(q)G(q_\nu^-)] = 0$ and $\lim_{q\to q_\nu^+}[G(q)-\eta(q)G(q_\nu^+)] = 0$, which smooth out the singularities at q_ν^- and q_ν^+, respectively, while the second and fourth terms [in Eq. (A8)] can be integrated analytically. We choose $\zeta(q) = \xi'(q)/\xi'(q_\nu^-)$ and $\eta(q) = \xi'(q)/\xi'(q_\nu^+)$. The integrals of the first and third terms are calculated by using the Gauss-Legendre quadrature method.

For half-space phonons, the electron wave vector at the threshold emission is $k_{\rm LO} = \sqrt{2m^*\omega_{\rm LO}/\hbar}$. Replacing k_ν in Eqs. (A2)–(A5) by $k_{\rm LO}$ then simply gives the limits of phonon wave vectors $q_{\rm LO}^-$, $q_{\rm LO}^+$ in the phonon emission and absorption cases. We find that the momentum relaxation rates are given by

$$\begin{aligned} \frac{1}{\tau_h} = &\frac{m^*}{2\pi\hbar^3}\frac{\gamma_{\rm LO}^2}{k}\left[N(\omega_{\rm LO}) + \frac{1}{2} \pm \frac{1}{2}\right]\int_{q_{\rm LO}^-}^{q_{\rm LO}^+}\frac{dq}{q}\mathcal{F}(q)\frac{1}{2k^2} \\ &\times (q^2 \pm k_{\rm LO}^2)\left\{1-\left[\frac{1}{2}\frac{k_{\rm LO}}{k}\left(\frac{q}{k_{\rm LO}} \pm \frac{k_{\rm LO}}{q}\right)\right]^2\right\}^{-1/2}. \end{aligned} \tag{A9}$$

These rates can be numerically calculated similar to the interface phonon rates $1/\tau_i$ above.

APPENDIX B: MOMENTUM RELAXATION RATES IN EXTREME QUANTUM LIMITS

Two limiting cases are of great interest: (i) When the electron kinetic energy $\mathcal{E}_{\mathbf{k}}$ is close to $\hbar\omega_{\rm LO}$ ($\hbar\omega_\nu$), a half-space (interface) phonon is emitted; (ii) when $\mathcal{E}_{\mathbf{k}}$ is close to zero, a half-space (interface) phonon is absorbed. These are referred to as the extreme quantum limits[2,3] in which analytical solutions exist for the electron-phonon scattering rate. Here, we attempt to obtain an analytical expression for the momentum relaxation rate for the limiting cases. To do this, deduction is illustrated in the following for half-space phonons, but solutions to the interface phonon scattering can be sought similarly, and rate expressions for both half-space and interface modes will be given. We first consider case (i), i.e., the threshold emission. We return to the original rate expression [Eq. (3)]. Insert the expression for matrix elements Eq. (5) into (3). For intrasubband processes, the energy terms in the δ function reduce to $\mathcal{E}_{\mathbf{k}'} - \mathcal{E}_{\mathbf{k}} + \hbar\omega_{\rm LO}$. The initial electron energy and wave vector are close to $\hbar\omega_{\rm LO}$ and $k_{\rm LO}$, respectively. Energy conservation requires that the final electron state is near the bottom of the subband, i.e., $k' \to 0$, and further momentum conservation finds the phonon wave vector $q \to k_{\rm LO}$. This results in the fractional increase of momentum being -1. It follows that the product of the δ functions, namely, $\delta(\mathcal{E}_{\mathbf{k}'} - \mathcal{E}_{\mathbf{k}} + \hbar\omega_{\rm LO})\delta_{\mathbf{k}',\mathbf{k}-\mathbf{q}}$ in Eq. (3) can be simply approached by

$\delta(\mathcal{E}_{\mathbf{k}'} - \mathcal{E}_{\mathbf{k}} + \hbar\omega_{\mathrm{LO}})\delta_{\mathbf{q},\mathbf{k}}$. The summation over $\mathbf{q}$ is then carried out, followed by the summation over $\mathbf{k}'$, which is converted to an integral as usual. Thus, we obtain the momentum relaxation rate for threshold emission

$$\left(\frac{1}{\tau_h}\right)_{\mathrm{th}} = \frac{\pi}{2} W_0 [N(\omega_{\mathrm{LO}}) + 1]\mathcal{F}(k_{\mathrm{LO}}), \tag{B1}$$

where W_0 is the basic rate $W_0 = \frac{e^2}{\hbar}\sqrt{2m^*\omega_{\mathrm{LO}/\hbar}}(\frac{1}{\epsilon_\infty} - \frac{1}{\epsilon_0})$. The momentum relaxation rate $(\frac{1}{\tau_h})_{\mathrm{th}}$ is in fact equal to the threshold electron-phonon scattering rate.[12] For interface phonons, the threshold rate can be written as

$$\left(\frac{1}{\tau_i}\right)_{\mathrm{th}} = \frac{\pi}{2} W_0 \sum_\nu \sqrt{\frac{\omega_\nu}{\omega_{\mathrm{LO}}}}\frac{\epsilon_{\mathrm{LO}}}{\epsilon_\nu}[N(\omega_\nu) + 1] f(k_\nu), \tag{B2}$$

where ϵ_{LO} and ϵ_ν are given by $\frac{1}{\epsilon_{\mathrm{LO}}} = \frac{1}{\epsilon_\infty} - \frac{1}{\epsilon_0}$ and $\frac{1}{\epsilon_\nu} = 2/[\beta^{-1}(\omega_\nu) + \bar{\beta}^{-1}(\omega_\nu)]$, respectively.

We now look at case (ii). Since momentum relaxation arises from a decrease in momentum, clearly one requires that the initial momentum $\hbar k \neq 0$. Mathematically, this is in accord with the expression for the fractional increase of momentum, which contains $1/k^2$. Recall, however, that we tackle the $k \to 0$ phonon absorption case; that is, both the denominator and numerator of the fractional increase of momentum approach zero. This is quite different from the phonon emission case, and an analytical solution can not be sought in the direct manner above. We turn to Eq. (A9) for half-space phonons. Let the integral in this $\frac{1}{\tau_h}$ expression be denoted by I_{LO}, which depends on k, i.e., $I_{\mathrm{LO}}(k)$. Change the variable of integration by using $q = kx + \sqrt{k^2 + k_{\mathrm{LO}}^2}$, such that the new variable of integration x is dimensionless ($x \in [-1,1]$) and the k's contained in the original limits of integration q_{LO}^-, q_{LO}^+ are transferred into the integrand. For simplicity, we denote the integrand by $g(k,x)$. As $k \ll k_{\mathrm{LO}}$, then the integrand $g(k,x)$ can be expanded into a Maclaurin series of powers of k, i.e., $g(k,x) = g(0,x) + g'(0,x)k + \frac{1}{2}g''(0,x)k^2 + \cdots$. Accordingly, the integral $I_{\mathrm{LO}}(k)$ can be simply expressed as $I_{\mathrm{LO}}(k) = \int_{-1}^{1} g(0,x)dx + k\int_{-1}^{1} g'(0,x)dx + O(k^2)$. It turns out that $g(0,x)$ is an odd function of x [thus making the first term in the $I_{\mathrm{LO}}(k)$ expression vanish] and $g'(0,x)$ is an even function of x. Recalling that in the $\frac{1}{\tau_h}$ expression there is a k-dependent factor $1/k$ in front of $I_{\mathrm{LO}}(k)$, in the limit of $k \to 0$, therefore, only the second term of $I_{\mathrm{LO}}(k)$ contributes for momentum relaxation. One finds that the final momentum relaxation rate can be expressed in a simple form in terms of the logarithmic derivative of the form factor as

$$\left(\frac{1}{\tau_h}\right)_0 = \frac{\pi}{4} W_0 N(\omega_{\mathrm{LO}})\mathcal{F}(k_{\mathrm{LO}})\left[1 + k_{\mathrm{LO}}\frac{\mathcal{F}'(k_{\mathrm{LO}})}{\mathcal{F}(k_{\mathrm{LO}})}\right]. \tag{B3}$$

For the momentum relaxation due to interface phonons, one starts with Eq. (A6) (use the lower signs for phonon absorption), repeats the process as before, and obtains the MRR expression for $k \to 0$:

$$\left(\frac{1}{\tau_i}\right)_0 = \frac{\pi}{4} W_0 \sum_\nu \sqrt{\frac{\omega_\nu}{\omega_{\mathrm{LO}}}}\frac{\epsilon_{\mathrm{LO}}}{\epsilon_\nu} N(\omega_\nu) f(k_\nu)\left[1 + k_\nu \frac{f'(k_\nu)}{f(k_\nu)}\right]. \tag{B4}$$

From Eq. (B3), clearly the sign of the $(\frac{1}{\tau_h})_0$ rate value is determined by the quantity in the square brackets. Using Eq. (11), it is found that, for any wave vector q,

$$1 + q\frac{\mathcal{F}'(q)}{\mathcal{F}(q)} = \frac{2b^2}{b+q}\frac{33b^3 + 15b^2q + 7bq^2 + q^3}{33b^4 + 54b^3q + 44b^2q^2 + 18bq^3 + 3q^4} > 0. \tag{B5}$$

Therefore, the momentum relaxation rate $(\frac{1}{\tau_h})_0$ due to half-space phonons always has a positive value. For interface phonons, we find that

$$1 + q\frac{f'(q)}{f(q)} = \frac{b - 5q}{b+q}, \tag{B6}$$

the sign of which is determined by $b - 5q$. Therefore, when the critical wave vector satisfies $k_\nu > b/5$, the interface modes of frequency ω_ν contribute a negative MRR.

For the *usual* electron-phonon scattering rate, however, the situation is different as the initial electron state can be *exactly* at the bottom of the subband $k = 0$. Then, the analytical solution can be obtained in a direct manner by using the approach $\delta(\mathcal{E}_{\mathbf{k}'} - \mathcal{E}_{\mathbf{k}} - \hbar\omega_{\mathrm{LO}})\delta_{\mathbf{k}',\mathbf{k}+\mathbf{q}} = \delta(\mathcal{E}_{\mathbf{k}'} - \mathcal{E}_{\mathbf{k}} - \hbar\omega_{\mathrm{LO}})\delta_{\mathbf{q},\mathbf{k}'}$, similar to that used in case (i) above. The scattering rate is $W_{h,0} = \frac{\pi}{2} W_0 N(\omega_{\mathrm{LO}})\mathcal{F}(k_{\mathrm{LO}})$ for half-space phonons and $W_{i,0} = \frac{\pi}{2} W_0 \sum_\nu \sqrt{\frac{\omega_\nu}{\omega_{\mathrm{LO}}}}\frac{\epsilon_{\mathrm{LO}}}{\epsilon_\nu} N(\omega_\nu) f(k_\nu)$ for interface phonons. It is readily found from Eq. (B5) that $\frac{1}{2}[1 + q\frac{\mathcal{F}'(q)}{\mathcal{F}(q)}] - 1 < 0$ and, thus, the momentum relaxation rate $(\frac{1}{\tau_h})_0$ is always smaller than the scattering rate $W_{h,0}$. For interface phonons, similarly, one finds from Eq. (B6) that $\frac{1}{2}[1 + q\frac{f'(q)}{f(q)}] - 1 < 0$ and, therefore, $(\frac{1}{\tau_i})_0 < W_{i,0}$.

*jian-zhong.zhang@hull.ac.uk

[1] B. K. Ridley, *Quantum Processes in Semiconductors* (Clarendon, Oxford, 1999).

[2] F. A. Riddoch and B. K. Ridley, J. Phys. C: Solid State Phys. **16**, 6971 (1983).

[3] B. K. Ridley, J. Phys. C: Solid State Phys. **15**, 5899 (1982).

[4] D. R. Anderson, N. A. Zakhleniuk, M. Babiker, B. K. Ridley, and C. R. Bennett, Phys. Rev. B **63**, 245313 (2001).

[5] B. K. Ridley, B. E. Foutz, and L. F. Eastman, Phys. Rev. B **61**, 16862 (2000).

[6] S. Das Sarma, J. K. Jain, and R. Jalabert, Phys. Rev. B **41**, 3561 (1990).

[7] S. D. Sarma and B. A. Mason, Ann. Phys. (NY) **163**, 78 (1985).

[8] H. Rücker, E. Molinari, and P. Lugli, Phys. Rev. B **45**, 6747 (1992).

[9] J.-Z. Zhang, B.-F. Zhu, and K. Huang, Phys. Rev. B **59**, 13184 (1999).

[10] B. C. Lee, K. W. Kim, M. Dutta, and M. A. Stroscio, Phys. Rev. B **56**, 997 (1997).

[11] N. Mori and T. Ando, Phys. Rev. B **40**, 6175 (1989).

[12] A. Dyson and B. K. Ridley, J. Appl. Phys. **109**, 054509 (2011).

[13]D. R. Anderson, M. Babiker, C. R. Bennett, and M. I. J. Probert, Phys. E (Amsterdam) **17**, 272 (2003).
[14]A. Dyson and B. K. Ridley, J. Appl. Phys. **108**, 104504 (2010).
[15]O. Ambacher *et al*., J. Appl. Phys. **87**, 334 (2000).
[16]O. Ambacher *et al*., J. Phys.: Condens. Matter **14**, 3399 (2002).
[17]F. F. Fang and W. E. Howard, Phys. Rev. Lett. **16**, 797 (1966).
[18]F. Stern and W. E. Howard, Phys. Rev. **163**, 816 (1967).
[19]B. K. Ridley, Semicond. Sci. Technol. **19**, 446 (2004).
[20]T. Ando, A. B. Fowler, and F. Stern, Rev. Mod. Phys. **54**, 437 (1982).
[21]D. R. Anderson, M. Babiker, C. R. Bennett, N. A. Zakhleniuk, and B. K. Ridley, J. Phys.: Condens. Matter **13**, 5999 (2001).
[22]J. C. Nipko and C.-K. Loong, Phys. Rev. B **57**, 10550 (1998).
[23]C. Bulutay, B. K. Ridley, and N. A. Zakhleniuk, Phys. Rev. B **62**, 15754 (2000).
[24]C. Bulutay, B. K. Ridley, and N. A. Zakhleniuk, Phys. B (Amsterdam) **314**, 63 (2002).
[25]B. K. Ridley, *Electrons and Phonons in Semiconductor Multilayers* (Cambridge University Press, Cambridge, 2009).
[26]F. A. Riddoch and B. K. Ridley, Surf. Sci. **142**, 260 (1984).
[27]J. H. Leach *et al*., Appl. Phys. Lett. **96**, 133505 (2010).
[28]M. A. Stroscio and M. Dutta, *Phonons in Nanostructures* (Cambridge University Press, Cambridge, 2001).
[29]L. F. Register, Phys. Rev. B **45**, 8756 (1992).